Archives of Environmental Protection
Vol. 52 no. 1 pp. 16–27

PL ISSN 2083-4772
DOI: 10.24425/aep.2026.158380

Zeolite-hydrogel composites for lithium and arsenic extraction from geothermal waters

Milena Koza*, Mentari Mukti, Barbara Tomaszewska

AGH University of Krakow, Poland

*Corresponding autor`s e-mail: milenakoza@agh.edu.pl

Keywords: zeolite, ion exchange, geothermal water, lithium extraction

Abstract: The rapid increase in lithium demand, driven by the growth of electric vehicles and energy storage systems, has raised concerns about future supply. To support the lithium supply chain, it is necessary to explore new sources, one of which is geothermal water. In this study, we review the current state of adsorption methods for lithium extraction from geothermal water and present our own approach. A zeolite-hydrogel composite was prepared using natural clinoptilolite, sodium alginate, and chitosan through a direct mixing method. Adsorption tests were performed using untreated geothermal water from the Dieng Geothermal Power Plant in Central Java to reflect natural conditions. The material's performance was evaluated by comparing ICP-MS analysis results of the water before and after adsorption. The results showed no significant reduction in lithium content. However, the use of 1.5 g of the composite, prepared from 5 g of clinoptilolite and a solution containing 0.5% sodium alginate and 0.5% chitosan- reduced arsenic concentration by approximately 52%. To enhance lithium adsorption, further optimization is required, including pH adjustment, silica removal, or modification of the composite structure. Further research is also needed to further explore the material's potential for arsenic removal.

Introduction

The strategic importance of lithium in the 21st century derives from its central role in electrochemical energy storage. Lithium-ion batteries (LIBs), with their high gravimetric and volumetric energy densities, are indispensable to electric vehicles (EVs), portable electronics, and renewable energy storage systems (Balaram et al., 2024; Hasan et al., 2025). In 2022, 80% of produced lithium was consumed in battery manufacturing, and EV deployment is expected to increase eightfold by 2030 (Balaram et al., 2024). According to the Global Critical Minerals Outlook (IEA, 2024), lithium demand is projected to rise tenfold by 2050 under a net-zero scenario. This trend creates an urgent need for scalable and environmentally sustainable lithium recovery methods, as well as diversification of supply beyond conventional sources (hard-rock and salar brine sources) toward unconventional but scalable reserves, such as geothermal brines.

Lithium reserves are unevenly distributed worldwide, with significant deposits in South America, the USA, Australia, and China (Yang et al., 2025). Figure 1 compares lithium reserves by country with their respective shares of global lithium production. Lithium resources are commonly classified into three groups: hard-rock minerals, continental brines, and secondary resources such as recycled batteries (Balaram et al., 2024). Among these, geothermal brines are emerging as a promising unconventional source of energy. Unlike seawater, where lithium concentrations are prohibitively low, geothermal brines often contain extractable lithium grades and can be valorized alongside geothermal heat and power production, resulting in favorable economics (Mojid et al., 2024). In addition, geothermal brines offer sustainability advantages, as they are by-products of geothermal energy generation. However, their high salinity, silica scaling, and complex multi-ion chemistry pose significant challenges for selective lithium extraction (Lee & Chung, 2022). Furthermore, integrating lithium recovery with geothermal operations has the potential to offset costs, enhance resource efficiency, and reduce environmental footprint.

Lithium can be recovered via precipitation, solvent extraction, electrochemical processes, membrane processes, and adsorption (Chen et al., 2021). Membrane-based approaches, including nanofiltration (NF), electrodialysis (ED), and capacitive deionization (CDI), have made significant progress (Tufa et al., 2025). NF membranes utilize size sieving and Donnan exclusion, a process by which ions are repelled from a charged membrane, to separate lithium from multivalent ions (Zavahir et al., 2021; Li et al., 2025). ED enables energy-efficient separation through ion-exchange membranes (Suu et al., 2025). CDI and its variants (MCDI, FCDI) have been praised for their low cost and environmental friendliness, although fouling and long-term stability remain obstacles (Yuan et al., 2025).

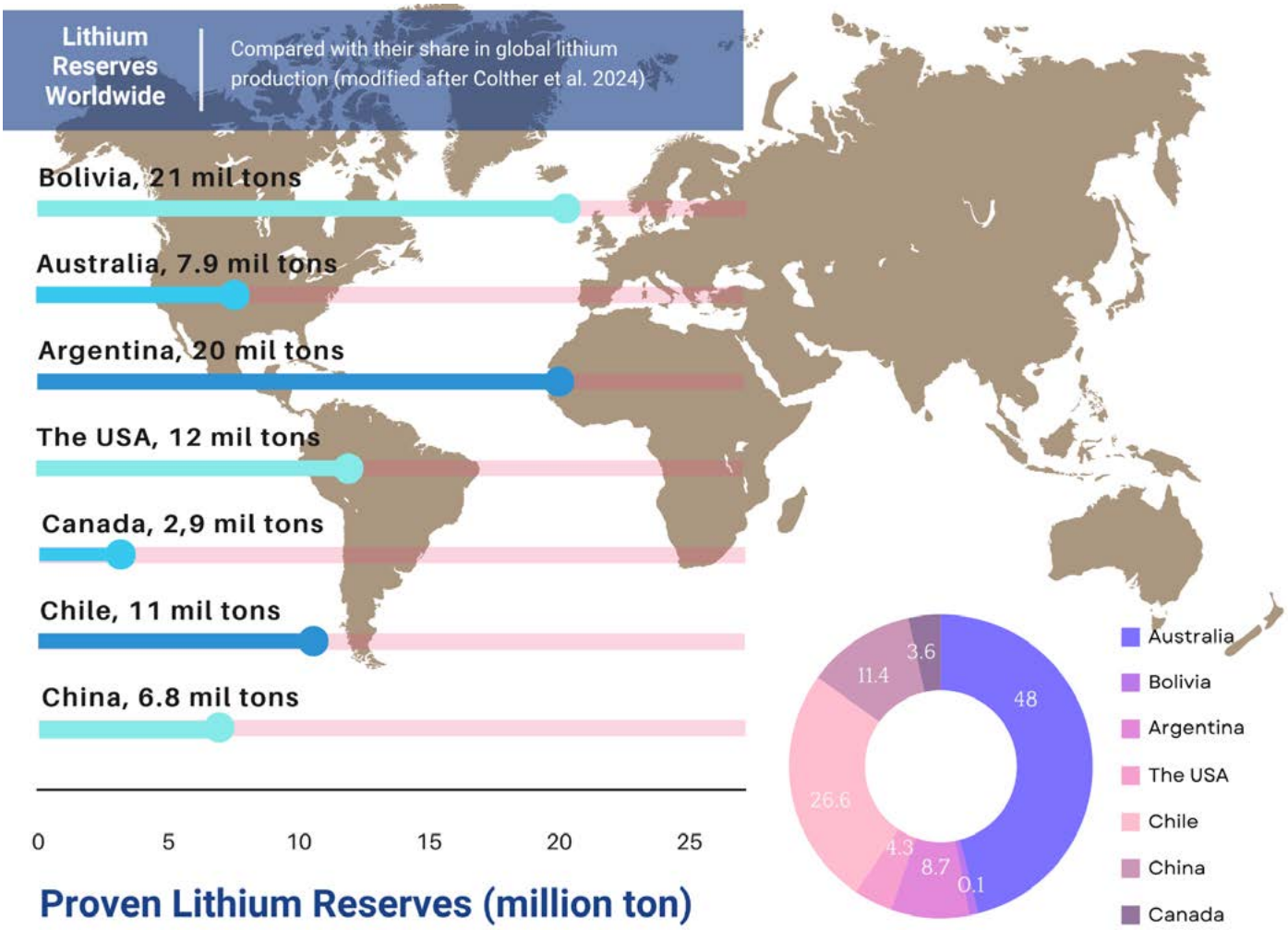

Fig 1. The size of lithium reserves by country, compared with their share in global lithium production (modified after Colther et al. 2024)

While various extraction techniques exist, adsorption is particularly attractive for its operational simplicity and potential for cost-effectiveness at scale (Mojid et al., 2024). Among adsorbents, inorganic lithium-ion sieves (LIS) based on manganese (LMO) or titanium (LTO) oxides have dominated research due to their high selectivity and reusability (Mends & Chu, 2023). Although these materials offer high capacities (>20 mg/g), they face significant challenges, including structural instability and manganese dissolution in LMO types, slower kinetics in LTO types, and more general issues related to regeneration costs and co-uptake of impurities (Weng et al., 2020; Zhou et al., 2025; Herrmann et al., 2022). Other inorganic adsorbents, such as metal-organic frameworks (MOFs), hydrogels, and zeolites, have attracted attention due to their tunable pore structures and high surface areas (Miao et al., 2022). Biological adsorbents, including bacteria capable of lithium accumulation, remain largely experimental (Zhou et al., 2025).

This has spurred interest in alternative, eco-friendly adsorbents. While research on individual components exists, studies on composite materials specifically designed for the complex matrix of geothermal brine remain limited. Previous work has explored both natural and synthetic zeolites for lithium adsorption, including clinoptilolite and zeolite 13X. Reich et al. (2023) reported that zeolite 13X can sorb up to 20.3 mg/g in synthetic LiCl solutions, but exhibits poor selectivity in natural geothermal brines, preferentially binding Ca, K, Sr, and As. Wiśniewska et al. (2018) compared synthetic Na-X and natural clinoptilolite using geothermal brine from Poland and demonstrated a strong pH dependence: adsorption was negligible at pH 5.5 but reached 100% lithium removal at pH 9 with clinoptilolite and PAA composites. Farhadi et al. (2019) enhanced clinoptilolite selectivity through crown ether modification, although testing was limited to seawater. A key limitation of these and many other studies is the predominant use of synthetic single-solute solutions, which fail to replicate the complex ion interference and scaling behavior of real geothermal water.

Furthermore, the potential of biopolymer hydrogels, such as chitosan and sodium alginate, has emerged as effective binders and modifiers. Recepoğlu et al. (2024) demonstrated that coating $LiMn_2O_4$ spinel with chitosan improved lithium uptake but reduced long-term stability. Abdelrahman et al. (2025) reported that alginate–graphene–MXene hydrogels achieved adsorption capacities exceeding 35 mg/g^{-1}, exhibiting high selectivity in multi-ion solutions. However, these studies relied on synthetic brines, leaving performance in authentic geothermal systems largely unexplored. Parallel research

indicates that chitosan and alginate hydrogels are highly effective for arsenic removal, a contaminant often found in geothermal fluids. For instance, Kang et al. (2019) used alginate–aluminum sludge beads, Zeng et al. (2024) tested chitosan composites, and Wu et al. (2025) developed zeolite–biochar hybrids, all of which proved effective in arsenic mitigation.

Moreover, as demonstrated in the works of Ningrum et al., chitosan-based hydrogels exhibit thermosensitivity, tunable porosity, and reversible adsorption–desorption cycles, which have been validated in chemically complex electroplating effluents (Ningrum et al., 2020, 2022, 2024). These systems, while not tested using geothermal water, share a key similarity: they involve multi-ionic, high-strength wastewaters in which selectivity, durability, and environmental safety are critical. The effective performance of chitosan hydrogels in such harsh matrices provides strong indirect evidence of their suitability for geothermal brines. Importantly, chitosan's functional amino groups (–NH_2) act as protonatable sites that strongly bind oxyanions, such as arsenate, while hydroxyl groups (–OH) contribute to hydrogen bonding and metal ion coordination (Liu et al., 2025). This dual chemistry enables chitosan to function both as a binder, enhancing the mechanical integrity of zeolite–alginate gels, and as an active sorption medium capable of targeting contaminants that co-occur with lithium.

However, the strategic combination of a low-cost, ion-exchange substrate (clinoptilolite zeolite) with these biopolymers into a single composite for geothermal brine applications has not been thoroughly investigated. Their complementary properties justify this combination: clinoptilolite provides a stable, porous framework and a source of cross-linking cations (Ca^{2+}), sodium alginate offers gelling capability and additional binding sites, and chitosan contributes high porosity and a strong affinity for contaminants (Liu et al., 2025; Miao et al., 2022). Together, they form a biodegradable, non-toxic composite with multifunctional potential. Whereas zeolite 13X and clinoptilolite rely primarily on size exclusion and ion-exchange mechanisms, chitosan introduces organic functionality that complements inorganic frameworks. Its inclusion transforms the composite from a purely inorganic ion-exchanger into a hybrid bio-inorganic adsorbent capable of lithium uptake, arsenic mitigation, and structural reinforcement.

The present work differs from FeOOH or MnO_2/TiO_2 lithium ion sieves. LIS materials are engineered for high selectivity but require acid regeneration and are prone to structural degradation (Herrmann et al., 2022; Weng et al., 2020). FeOOH and related oxides exhibit strong sorption through their hydroxyl-rich surfaces, but they lack the biodegradability and benign disposal profile of biopolymer composites (Disu et al., 2024). Chitosan, in contrast, represents an eco-functional choice: it may not maximize Li uptake compared to LIS, but it balances adsorption potential with environmental safety, low production cost, and operational versatility, while also functioning as a pretreatment medium that reduces arsenic and conditions brine for downstream separation. Thus, the inclusion of chitosan, alongside clinoptilolite and alginate, is a deliberate choice to advance a sustainable, multifunctional,

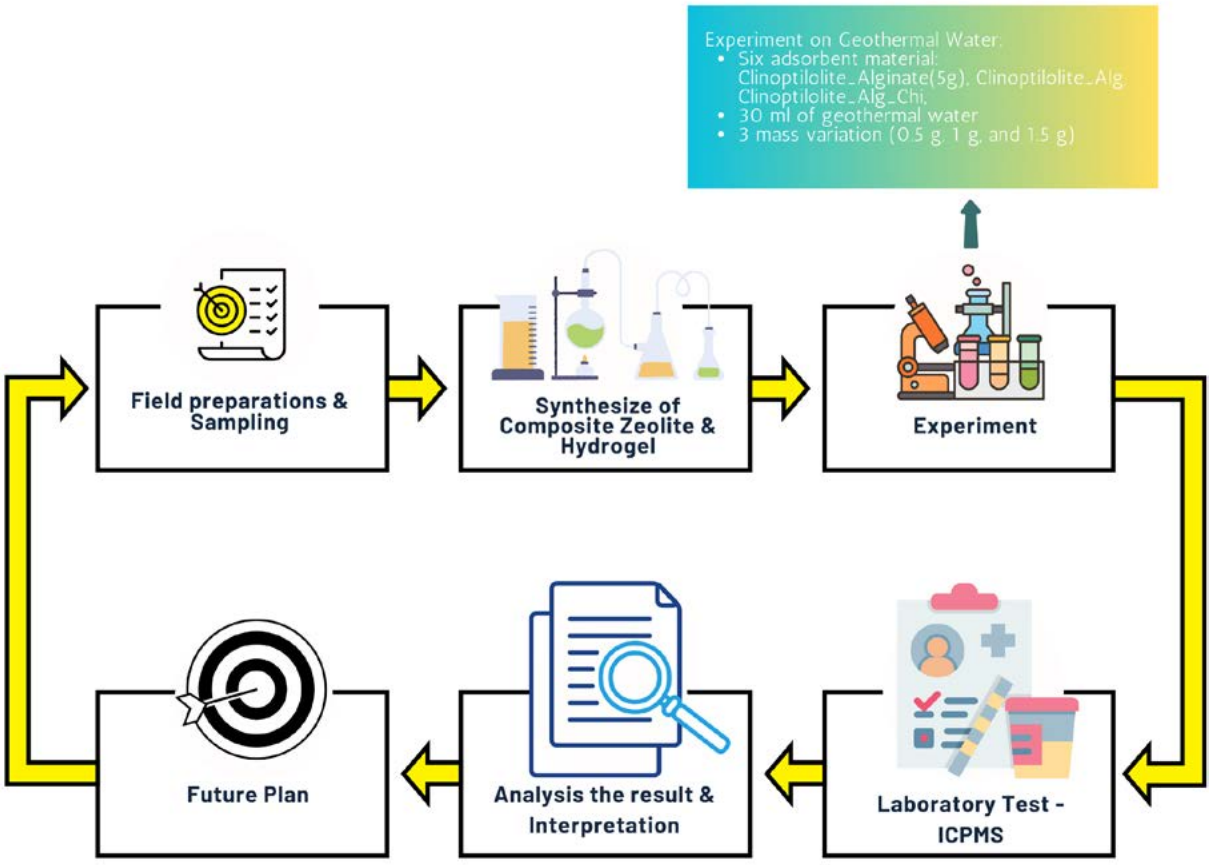

Fig 2. Schematic Diagram of The Experiment

and environmentally responsible approach to lithium recovery.

This paper introduces a new approach to lithium adsorption from geothermal brines by combining natural zeolite, sodium alginate, and chitosan into composite materials. Although these materials exhibit favorable properties for lithium adsorption, their combined performance has not been thoroughly investigated. The study differs from previous research on zeolite-based adsorbents by using natural geothermal water for adsorption tests. Real geothermal brines generally have a more complex chemical composition than synthetic solutions, which is critical for assessing the practical applicability of such materials.

Materials and methods

Geothermal water characterization

In this research, natural geothermal water from the Dieng Geothermal Power Plant in Java, Indonesia, was used. A total of 6 L of water was collected from Well Pad 28A. The pH of the geothermal water during sampling was 6.5. The sample was then transported to the laboratory at the Faculty of Geology, Geophysics, and Environmental Protection, AGH University of Krakow, Poland. Figure 2 illustrates the experimental methodology.

The physicochemical characterization of the brine was conducted by the accredited Laboratory of Hydrogeochemistry. The pH and total mineralization were measured upon arrival. The elemental composition was determined using inductively coupled plasma mass spectrometry (ICP-MS) on a Thermo Scientific iCAP RQ instrument (Thermo Fisher Scientific Inc., USA). The ICP-MS system was equipped with a concentric glass nebulizer, a Peltier-cooled quartz cyclonic spray chamber (maintained at 3 °C), and a demountable quartz torch. The analysis was performed in Helium kinetic energy discrimination (He-KED) mode to mitigate polyatomic interferences. The instrument was operated at an RF power of 1550 W, and a "high matrix" insert was used to accommodate the high total dissolved solids (TDS) content. The system was calibrated using a multi-element standard solution, and rhodium (Rh) was used as an internal standard to correct for signal drift and matrix effects.

Table 1. Concentrations of selected cations in geothermal water from the Dieng Geothermal Power Plant

Cation	mg/L	mval/L	% mval
As^{3+}	63.51 ± 0.71	2.544	0.443
Ca^{2+}	974.9 ± 3.5	48.650	8.467
K^{+}	3091 ± 18	79.056	13.76
Li^{+}	55.02 ± 0.15	7.928	1.38
Mn^{2+}	12.55 ± 0.44	0.457	0.08
Na^{+}	10020 ± 40	435.661	75.826
Sr^{2+}	7.82 ± 0.11	0.178	0.031

The analysis revealed a high-salinity brine with a total mineralization of 39.02 g/L and an initial pH of 6.5. The brine was characterized by a high lithium concentration and an exceptionally low Mg^{2+}/Li^{+} mass ratio of 0.015, making it a theoretically favorable candidate for lithium recovery. The complete elemental composition of the major cations is presented in Table 1.

Adsorbent preparation

Natural clinoptilolite from a Slovakian deposit was used as the base adsorbent material. It was manually ground using an agate mortar and pestle to obtain a fine, homogeneous powder. Three composite adsorbents were prepared using a direct mixing method:

- Variant I: 5 g clinoptilolite + 25 mL of a 5% (w/v) sodium alginate solution.
- Variant II: 5 g clinoptilolite + 25 mL of a 1% (w/v) sodium alginate solution.
- Variant III: 5 g clinoptilolite + 25 mL of a solution containing 0.5% (w/v) sodium alginate and 0.5% (w/v) chitosan.

The mixtures were combined in 120 mL polypropylene containers and agitated on an orbital shaker (300 rpm) for 24

Table 2. Exact mass of every batch of adsorbent used in adsorption tests

		MASS (g)			WATER VOLUME	pH
		CP+A5%	CP+A1%	CP+A+CH		
VARIANT I (ADSORBENT MASS= 1g)	SAMPLE 1	1.0026	1.0297	1.0417	30 mL	6.12
	DUPLICATE	1.0227	1.0685	1.0131		
VARIANT II (ADSORBENT MASS= 1.5g)	SAMPLE 1	1.5100	1.5048	1.5019		
	DUPLICATE	1.5254	1.5067	1.5146		
VARIANT III (ADSORBENT MASS= 0.5g)	SAMPLE 1	0.5092	0.5019	0.5157		
	DUPLICATE	0.5063	0.5110	0.5056		

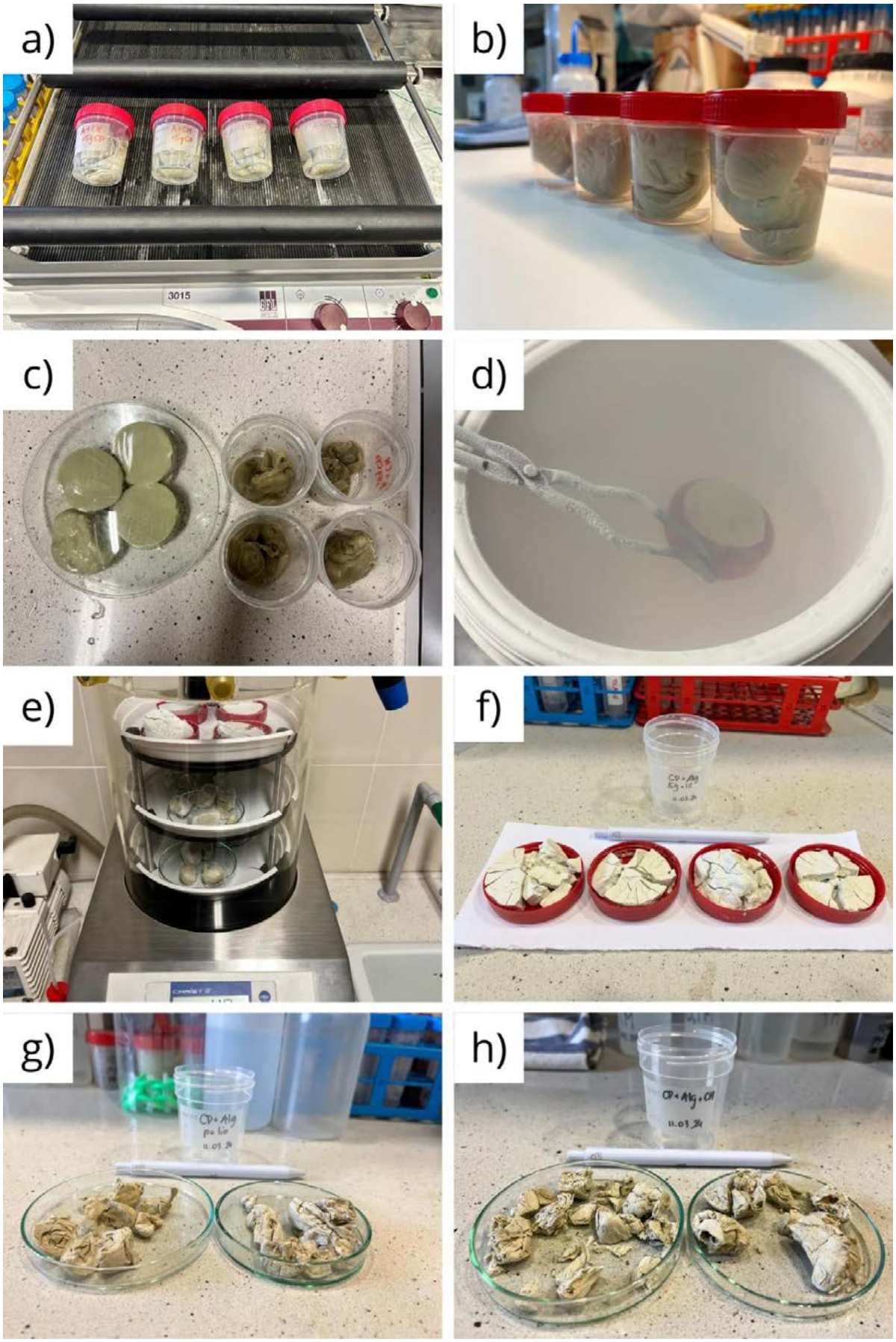

Fig 3. Stages of zeolite-hydrogel composite preparation: a) Gel formation process in an orbital shaker; b) Samples obtained as a result of crosslinking process; c) Division of the material into smaller parts; d) Freezing of the samples in liquid nitrogen; e) Freeze-drying of the materials; f) Ready-to-use composite 5g CP+ 1% Na-Alg; g) Ready-to-use composite 5g CP+ 5% Na-Alg; h) Ready-to-use composite 5g CP+ 0.5% Na-Alg+ 0.5% chitosan

hours at room temperature to ensure homogenization and cross-linking. The Ca^{2+} ions naturally present in the clinoptilolite structure facilitated the gelation of the sodium alginate. The resulting hydrogels were extracted, cut into smaller pieces (~5 mm), flash-frozen with liquid nitrogen, and lyophilized (freeze-dried) for 48 hours to obtain dry, porous composites. The preparation stages are depicted in Figure 3.

Adsorption experiments

Batch adsorption experiments were conducted to evaluate the performance of the composites. Pre-weighed masses of each freeze-dried composite (0.5 g, 1.0 g, and 1.5 g; exact masses are listed in Table 2) were placed in 50 mL polypropylene test tubes. A volume of 30 mL of the geothermal brine was added to each tube.

Before the experiment, the pH of the stored brine was re-measured and found to be 6.12; representing a slight decrease from the original value of 6.5, which was attributed to the precipitation of mineral phases observed at the bottom of the storage container. The pH was not adjusted to simulate real-world application conditions. The test tubes were sealed and placed on an orbital shaker for 24 hours at 300 rpm at room temperature (22 ± 2 °C) to ensure equilibrium was reached. After the contact period, the solutions were separated from the adsorbents by centrifugation followed by filtration through 0.45 µm disposable syringe filters with a cellulose acetate membrane. The filtrates were analyzed for their post-adsorption elemental composition using the same iCAP RQ ICP-MS method described in Section 3.1. The instrument's "high matrix" insert and He-KED mode were essential for accurate analysis of these complex, high-TDS solutions. The experimental setup is shown in Figure 4.

The adsorption efficiency of the prepared composites was assessed using two complementary parameters: adsorption capacity (Q, m/g) and removal efficiency (R, %). These indices are commonly employed in adsorption studies because they capture both the material's intrinsic uptake ability and its practical effectiveness in reducing contaminant levels from solution.

For a given element i, the adsorption capacity was calculated as:

$$Q_i = (C_0 - C_{Equ}) \cdot \frac{V}{m}$$

While the removal efficiency was determined using:

$$R\ (\%) = ((C_o - C_e) / C_o) \times 100$$

In this equation:

Qi – adsorption capacity [mg/g];

C0- initial concentration of the adsorbate [mg/L];

CEqu – concentration of the adsorbate after the adsorption process [mg/L];

V – volume of the solution [L];

m- adsorbent mass [g] (Reich et al. 2023).

Results and discussion

Adsorption Performance and Ion Selectivity

The adsorption experiments with clinoptilolite–hydrogel composites provided a comprehensive dataset for evaluating their performance in real geothermal brine (Dieng, Indonesia). The initial composition of the raw brine, determined by ICP–MS, was dominated by sodium (10.020 mg/L; 75.8% mval), followed by potassium (3.091 mg/L; 13.8% mval), calcium (974.9 mg/L; 8.5% mval), and arsenic (63.51 mg/L; 0.44%

Table 3. Results of the ICPMS analysis after the adsorption tests

Sample name	As	Ca	K	Li	Mn	Na	Sr
	[mg/L]						
I CP+A5	66.70	1105	2495	51.97	16.09	10093	9.04
I D CP+A5	69.11	1110	2552	52.26	16.15	10068	9.14
I CP+A+CH	57.38	3050	3055	55.47	16.86	10580	11.26
I D CP+A+CH	62.42	2966	3075	56.59	17.35	10679	11.44
I CP+A	55.57	2658	2961	54.92	17.30	10377	10.07
I D CP+A	55.46	2512	2939	54.18	17.41	10226	10.11
II CP+A5	67.96	1323	2437	56.00	16.36	10730	9.35
II D CP+A5	68.8	1297	2382	54.46	16.11	10479	9.25
II CP+A+CH	30.38	3269	2931	55.33	16.62	10446	11.43
II D CP+A+CH	51.61	3894	2956	55.48	17.13	10483	12.18
II CP+A	47.16	3266	2762	52.13	16.79	9881	10.28
II D CP+A	44.14	3413	2791	52.77	17.46	10004	10.81
III CP+A5	70.63	1041	2803	53.50	17.45	10106	9.71
III D CP+A5	70.85	1044	2843	54.55	17.53	10283	9.74
III CP+A+CH	66.15	1652	2990	54.20	16.99	10142	10.12
III D CP+A+CH	66.12	1933	3130	57.27	17.71	10668	10.77
III CP+A	62.91	1805	2977	52.78	17.49	10065	9.96
III D CP+A	59.52	1822	3013	54.29	17.61	10223	10.09

Table 4. Average values of Qi and R(%) for the major cations calculated for each type of adsorbent

Type of adsorbent	Cation						
	As	Ca	K	Li	Mn	Na	Sr
	Qi						
CP+A5%	-0.22	-1.37	12.72	0.04	-0.16	-7.99	-0.06
CP+A+CH	0.13	-54.05	1.86	-0.03	-0.17	-16.76	-0.11
CP+A1%	0.24	-48.64	5.43	0.05	-0.18	-4.77	-0.08
	R (%)						
CP+A5%	-8.66	-18.31	16.36	2.23	-32.39	-2.73	-19.85
CP+A+CH	12.33	-186.58	2.21	-1.27	-36.32	-4.79	-43.22
CP+A1%	14.77	-164.58	5.95	2.74	-38.21	-1.09	-30.69

mval). Lithium, though technologically critical, represented only 55.02 mg/L (1.38% mval), constituting a minor fraction of the total ionic composition.

Across the tested composites, adsorption capacities and removal efficiencies differed markedly between cations, reflecting both intrinsic material selectivity and the competitive dynamics of the multicomponent brine, as shown in Tables 3 and 4.

Lithium removal was consistently poor across all tested materials. Variant I (CP+A5%: 5 g clinoptilolite + 25 mL of 5% alginate solution) achieved the highest reduction, lowering lithium concentration from 55.02 mg/L to 51.97 mg/L, corresponding to a removal efficiency of 5.5% and an adsorption capacity of 0.09 mg/g^{-1}. Variants II and III exhibited even lower efficiencies (2.7% and negative values, respectively). In some trials with CP+A+CH (Variant III), lithium concentrations increased, suggesting desorption of Li^+ initially present in the zeolite framework. This outcome is consistent with literature reports. Reich et al. (2023) found that zeolite 13X exhibited negligible affinity for lithium in

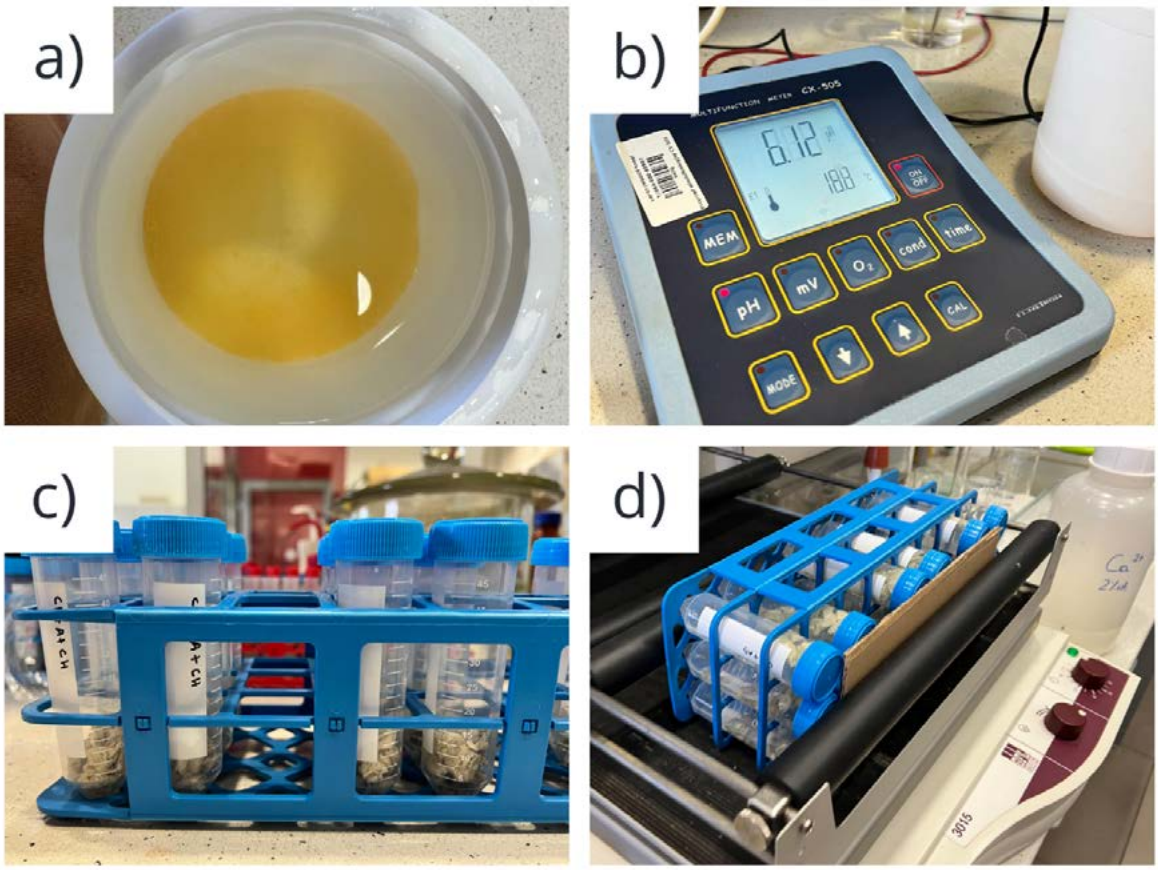

Fig 4. Photographic overview of the adsorption experiments: a) Precipitate settled at the bottom of the container used for storing geothermal water; b) pH of the water at the time of testing; c) Measured adsorbents in polypropylene test tubes; d) Adsorption test in an orbital shaker

geothermal brines, while Wiśniewska et al. (2018) showed that clinoptilolite preferentially adsorbs larger alkali metals over Li^+. The weak performance is fundamentally linked to lithium's high hydration energy (−520 kJ mol^{-1}) and kosmotropic nature, which hinders displacement from hydration shells and limits ion exchange with zeolitic sites. Figure 5 illustrates lithium concentrations after the adsorption tests for each studied material.

By contrast, potassium exhibited strong uptake across all variants. In Variant I, K^+ concentrations decreased from 3.091 to 2.495 mg/L (R = 16.4%; Q = 12.7 mg/g^{-1}). Potassium consistently showed the highest positive adsorption capacity among all ions studied. This preference reflects clinoptilolite's structural affinity for larger hydrated cations, which fit well into its exchange channels. Literature confirms that clinoptilolite naturally favors K^+, Cs^+, and Sr^{2+} over smaller alkali metals, a behavior rooted in both ionic size and hydration energetics (Wiśniewska et al., 2018).

Unexpectedly, sodium and calcium concentrations increased after treatment, yielding negative removal efficiencies. In Variant III, Na^+ concentrations rose from 10.020 to 10.580 mg/L (R = −4.8%), while Ca^{2+} increased from 974.9 to over 3.000 mg/L in several replicates (R = −186%). This phenomenon can be attributed to the leaching of framework-balancing ions from clinoptilolite. Both Na^+ and Ca^{2+} are intrinsic to the aluminosilicate lattice and readily undergo ion exchange under neutral pH conditions. Similar effects were reported by Farhadi et al. (2019), who found that unwashed clinoptilolite released Na^+ and Ca^{2+}, complicating adsorption balances unless the material was pretreated with neutral electrolytes.

A striking and unexpected finding was the significant reduction in arsenic concentration. In Variant III (CP+A+CH: clinoptilolite + alginate + chitosan), arsenic concentration decreased from 63.51 to 30.38 mg/L (R ≈ 52%, Q = 0.66 mg/g^{-1}). Variants I and II also exhibited partial arsenic removal (8–15%). This result is consistent with the functional chemistry of chitosan and alginate: the protonated amino groups of chitosan (pKa ≈ 6.3) bind anionic arsenate ($H_2AsO_4^-$), while alginate contributes carboxylate groups that stabilize oxyanion binding. Comparable findings were reported by Zeng et al. (2024) for chitosan-based composites and by Kang et al. (2019) for alginate–alum sludge beads.

The overall ion selectivity observed can be summarized as: K^+ > As(V) > Li^+ (marginal) ≫ Na^+, Ca^{2+} (desorption). This hierarchy reflects both the structural preferences of clinoptilolite and the thermodynamics of ion hydration. Potassium, being chaotropic and weakly hydrated, is favored; lithium, strongly kosmotropic, is disadvantaged; and sodium and calcium leach due to framework instability. These selectivity trends are consistent with hydration energetics and the Hofmeister series.

- Potassium (K^+): Weak hydration enthalpy (−322 kJ mol^{-1}), small hydration shell (~2.3 Å), chaotropic → easily exchanges into zeolite channels.
- Sodium (Na^+): Intermediate hydration enthalpy (−406 kJ mol^{-1}), hydration shell ~2.7 Å → moderately competitive but prone to desorption from framework.

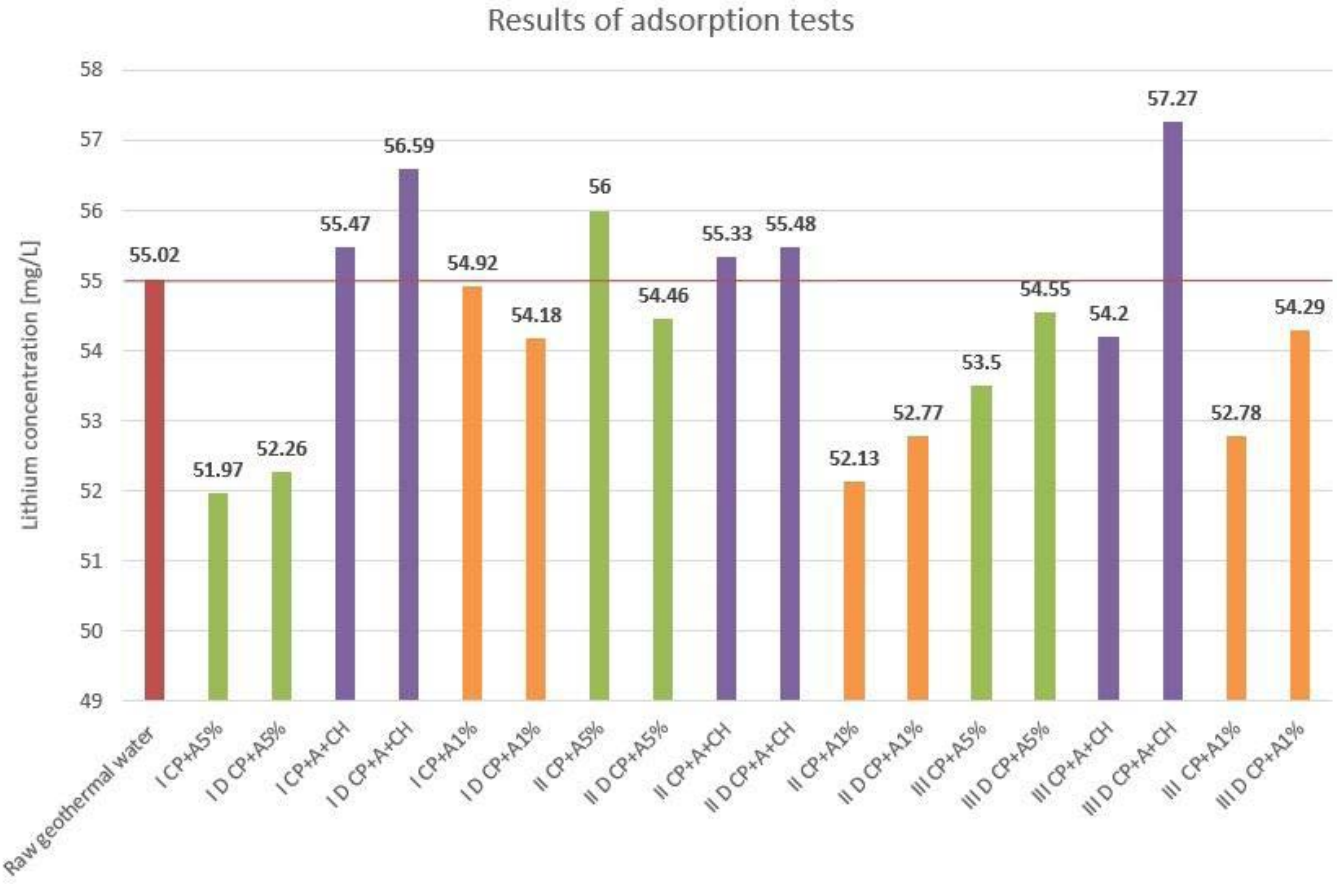

Fig 5. Lithium concentrations after the adsorption test for each composite

- Lithium (Li^+): Strong hydration enthalpy (−520 kJ mol^{-1}), large hydration shell (~3.8 Å), kosmotropic → poorly exchanges, sometimes desorbs.
- Calcium (Ca^{2+}): High charge density, tightly bound in the framework, but can leach under neutral pH conditions.
- Arsenic (As(V)): Exists as $H_2AsO_4^-$ at pH 6; strongly binds to protonated amines and carboxylate groups in hydrogels.

Figure 6 presents a graphical summary of ion selectivity trends in zeolite–hydrogel composites. Panel A shows experimental removal efficiencies plotted against hydration energy. The inverse relationship is evident: ions with lower hydration energies (e.g., K^+) were preferentially removed, while Li^+ was disadvantaged. Panel B illustrates these trends in the context of the Hofmeister series, emphasizing that ion selectivity is fundamentally governed by hydration thermodynamics. This mechanistic explanation underscores a critical point: lithium recovery from real brines faces intrinsic chemical barriers due to hydration energetics, which unmodified zeolites cannot overcome. As illustrated in Figure 6, these selectivity patterns are consistent with the removal efficiencies and hydration energetics of competing ions.

Influence of pH and Silica Interference

The chemical environment of the geothermal brine, particularly its pH and high silica content, significantly influenced the adsorption performance. The brine collected from the Dieng field had a pH of 6.5 at the time of sampling, which decreased slightly to 6.1 after batch contact with the composites. This near-neutral to mildly acidic range is unfavorable for lithium uptake. Numerous studies have shown that lithium recovery efficiency improves markedly under alkaline conditions. Wiśniewska et al. (2018) demonstrated that natural clinoptilolite removed nearly 100% of lithium from solution at pH 9, whereas removal was negligible at the natural brine pH of 5.5. Similarly, Mends and Chu (2023) reported that the deprotonation of surface hydroxyl groups at elevated pH increases the negative charge density on adsorbent surfaces, thereby promoting cation exchange and lithium sorption. In contrast, under acidic conditions, protons compete strongly with lithium for active sites, effectively suppressing adsorption and, in some cases, promoting desorption.

The variability in arsenic removal also reflects the influence of speciation. At pH ~6, arsenic may exist as both As(III) (predominantly neutral H_3AsO_3) and As(V) ($H_2AsO_4^-$). Chitosan exhibits limited affinity for neutral As(III) but shows strong electrostatic interactions with As(V). Thus, removal efficiency is likely higher in samples where a greater fraction of arsenic was present in the pentavalent form, possibly due to oxidation during sample handling or contact with trace dissolved oxygen. This observation suggests an important direction for future optimization: pre-oxidizing arsenic to As(V) (e.g., with H_2O_2 or aeration) could standardize speciation and enhance the reproducibility of arsenic uptake.

The slight decrease in pH during the experiments may have further exacerbated these effects. Acidification can occur due to ion exchange processes in which protons are released from zeolite or polymer functional groups during cation substitution. In the present study, this shift to pH 6.1 likely reinforced competitive proton binding, thereby reducing lithium accessibility to exchange sites. It is therefore plausible that the consistently low lithium removal efficiency observed across all composites was driven not only by the inherent selectivity of clinoptilolite but also by the unfavorable pH environment.

In addition to pH, the geothermal brine was characterized by substantial silica concentrations: 94.20 mg/L of SiO_2 and 122.47 mg/L of H_2SiO_3. High silica levels are a well-recognized operational challenge in geothermal systems, where they contribute to scaling and equipment fouling. In adsorption processes, dissolved and colloidal silica can deposit on sorbent surfaces, physically blocking active sites and reducing ion accessibility. Lee and Chung (2022) demonstrated in a solvent extraction study that silicate ions strongly interfered with the lithium separation from geothermal water, necessitating silica pretreatment to achieve meaningful recovery. Although that study employed a different separation mechanism, the implications for adsorption are similar: high silica levels can form protective coatings around sorbent particles or interact chemically with polymer matrices, thereby impairing adsorption efficiency.

In the case of hydrogel-modified composites, silica interference may be even more pronounced. Alginate gels rely on ionic crosslinking, typically with Ca^{2+}, to form their three-dimensional network structure. Silicic acid and colloidal silica can interact with these crosslinking sites or penetrate the gel matrix, leading to stiffening or pore blockage that reduces ion diffusion. Similarly, the amine groups of chitosan can form hydrogen bonds with silicic acid, potentially altering the accessibility of these functional groups for cation binding. Such interactions reduce the effectiveness of hydrogel modification in enhancing lithium uptake, further contributing to the poor performance observed. In regard to ion competitiveness, the Li/Na molar ratio was only 1.8%, highlighting lithium's disadvantage in multicomponent systems. Combined with its hydration barrier, this explains why Na^+ and K^+ dominated ion exchange, while Li^+ uptake remained negligible.

The combined influence of near-neutral pH and silica fouling provides a compelling explanation for the limited lithium adsorption achieved in this study. These factors are not unique to the Dieng brine but are common across many geothermal systems worldwide. Therefore, any adsorption-based lithium recovery strategy must incorporate pretreatment steps to optimize chemical conditions. Specifically, two interventions appear necessary: (i) pH adjustment to mildly alkaline conditions (pH 9–10), and (ii) silica removal, either through pH swing precipitation, seeded crystallization, or chemical additives that promote silica aggregation and settling. Without such pretreatment, lithium-selective adsorbents are unlikely to reach their theoretical performance, regardless of material design.

Conclusions

The present study investigated the adsorption performance of clinoptilolite–hydrogel composites, prepared with sodium alginate and chitosan, for the simultaneous removal of lithium and co-occurring ions from geothermal brines. The findings highlight both the limitations and the unexpected opportunities associated with these materials in the context of direct lithium extraction (DLE) and brine conditioning. The key findings may be summarized as follows:

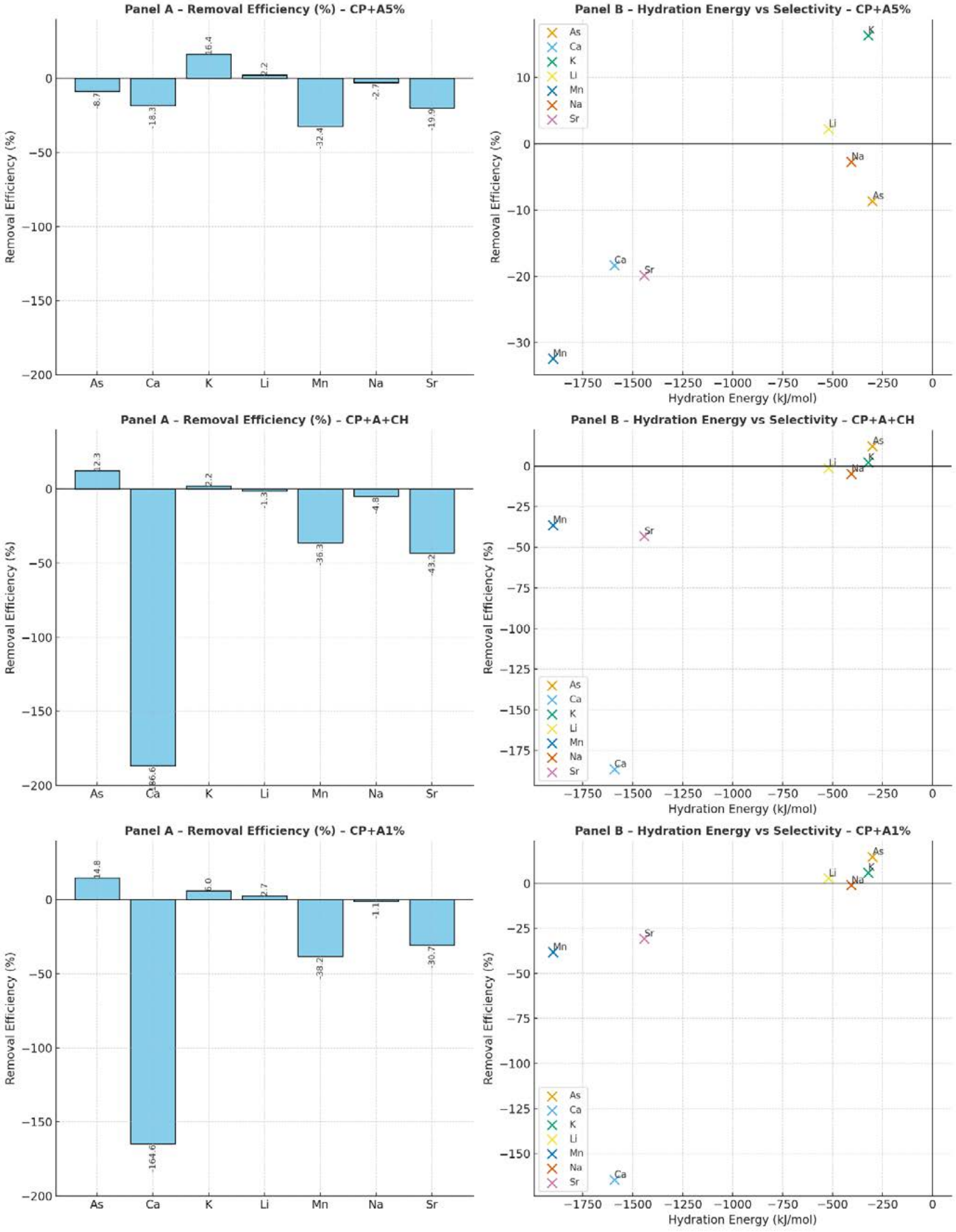

Fig 6. Ion selectivity trends in zeolite–hydrogel composites. Panel A displays removal efficiencies (%) for major ions; Panel B illustrates the relationship between hydration energy (kJ/mol) and ion selectivity, highlighting the Hofmeister effect

1. **Lithium Recovery Limitations.** Across all composite formulations tested, lithium adsorption was negligible. The maximum removal efficiency recorded was ~5.5% (Variant I: CP+A5%), corresponding to an adsorption capacity of only 0.09 mg/g^{-1}. In several instances, particularly with Variant III (CP+A+CH), the lithium concentration in solution increased relative to the untreated brine, indicating desorption of lithium originally present within the clinoptilolite structure. This outcome is consistent with the well-documented limitations of zeolites for lithium recovery: lithium's small hydrated radius and high hydration energy (−520 kJ mol^{-1}) make it a poor competitor in ion-exchange reactions compared with larger, weakly hydrated cations such as K^+ or Sr^{2+} (Reich et al., 2023; Wiśniewska et al., 2018).
2. **Environmental and Chemical Barriers.** The geothermal brine matrix itself imposed additional barriers. The mildly acidic to neutral pH (6.1–6.5) created conditions under which proton competition suppresses lithium binding, in agreement with prior studies showing that lithium uptake by natural zeolites is negligible below pH 7 but increases under alkaline conditions (Wiśniewska et al., 2018; Mends & Chu, 2023). Simultaneously, the high silica concentration (94.20 mg/L SiO_2 and 122.47 mg/L H_2SiO_3) likely caused pore blocking and site fouling, as has been observed in other geothermal systems where silica scaling impedes adsorption or solvent extraction (Lee & Chung, 2022). These results underline that adsorption-based lithium recovery cannot be decoupled from the geochemistry of the source fluid.
3. **Arsenic removal as a co-benefit.** An unexpected but significant finding was the substantial removal of arsenic, particularly in composites containing chitosan. Variant III (CP+A+CH) achieved ~52% reduction in arsenic concentration (63.51 → 30.38 mg/L), corresponding to an adsorption capacity of 0.663 mg/g^{-1}. This effect is attributable to the protonated amine groups of chitosan, which strongly interact with arsenate ($H_2AsO_4^-$) at near-neutral pH, and to the carboxylate groups of alginate, which further stabilize oxyanion binding (Zeng et al., 2024; Kang et al., 2019). While lithium removal was poor, the dual-function nature of the composites for simultaneous arsenic mitigation positions them as potential pretreatment materials in geothermal brine management.

Further Research

The limitations and co-benefits identified in this study highlight clear priorities for future research, both in material optimization and process design:

- **Brine pretreatment strategies:** To address the dual barriers of pH and silica, future experiments should incorporate systematic pH adjustment and silica removal. Alkalinization to pH 9–10 can increase surface deprotonation and enhance lithium uptake. Silica concentrations can be reduced through methods such as seeded precipitation or co-precipitation with magnesium hydroxide ($Mg(OH)_2$). Implementing these pretreatments would enable a more precise assessment of the intrinsic adsorption potential of the composites.
- **Material modification:** Incorporating iron oxyhydroxide (FeOOH) into the composite formulation represents a promising direction for future development. FeOOH polymorphs are abundant, environmentally benign, and offer a high density of hydroxyl groups capable of complexing with lithium ions. They also provide strong binding sites for arsenic, potentially enhancing the dual-function capacity of the composites. Preliminary formulations could include 15–25 wt.% FeOOH blended with clinoptilolite and alginate.
- **Optimization of biopolymer composition:** The ratio of alginate to chitosan requires systematic investigation. While alginate contributes structural integrity and cation exchange potential, chitosan is clearly more effective for arsenic removal. A factorial design varying alginate (0.5–5 wt.%) and chitosan (0.3–1 wt.%) would allow determination of the optimal balance for dual-function performance.
- **Kinetic and column studies:** All experiments reported here were conducted in batch mode with 24 h contact time. Kinetic studies with shorter contact times are necessary to determine adsorption rates and model mass transfer behavior. Furthermore, column experiments should be pursued to assess breakthrough curves, bed volumes, and regeneration performance, providing data relevant to real process design.
- **Speciation control for arsenic:** The variability in arsenic removal observed across replicates suggests sensitivity to As speciation. Since chitosan shows a higher affinity for As(V) than for As(III), pre-oxidizing arsenic to As(V) (e.g., using hydrogen peroxide or aeration) may enhance both the efficiency and reproducibility of removal. This step could be readily integrated into a pretreatment scheme with minimal added cost.

Acknowledgement

Research project was supported by the „Excellence Initiative – Research University" program at AGH University of Krakow, Poland.

References

Abdelrahman, N.S., Hong, S., Choi, D.S., Arafat, H.A. & AlMarzooqi, F. (2025). Interfacial adsorption and recovery of Lithium ions using sulfonated graphene oxide and $Ti_3C_2T_x$ MXene nanocomposite hydrogels. *Desalination* 606, 118766. DOI:10.1016/j.desal.2025.118766.

Balaram, V., Santosh, M., Satyanarayanan, M., Srinivas, N. & Gupta, H. (2024). Lithium: A review of applications, occurrence, exploration, extraction, recycling, analysis, and environmental impact. *Geoscience Frontiers* 15, 101868. DOI:10.1016/j.gsf.2024.101868.

Chen, S., Chen, Z., Wei, Z., Hu, J., Guo, Y. & Deng, T. (2021). Titanium-based ion sieve with enhanced post-separation ability for high performance lithium recovery from geothermal water. *Chemical Engineering Journal* 410, 128320. DOI:10.1016/j.cej.2020.128320.

Disu, B., Rafati, R., Haddad, A.S., Roca,J.A.M., Clar, M.I.I. & Bakhtiari, S.S.E. (2024). Review of recent advances in lithium extraction from surface brines. *Geoenergy Science and Engineering* 241, 213189. DOI:10.1016/j.geoen.2024.213189.

Farhadi, M., Rashidi, A. & Mallah, M.H. (2019). Analysis of lithium separation by modified zeolite using fuzzy logic: equilibrium,

kinetics and thermodynamic. *Desalination and Water Treatment* 148, 141-151. DOI:10.5004/dwt.2019.23832.

Hasan, M.M., Haque, R., Jahirul, M.I., Rasul, M.G., Fattah, I.M.R., Hassan, N.M.S. & Mofijur, M. (2025). Advancing energy storage: The future trajectory of lithium-ion battery technologies. *Journal of Energy Storage* 120, 116511. DOI:10.1016/j.est.2025.116511.

Herrmann, L., Ehrenberg, H., Graczyk-Zajac, M., Kaymakci, E., Kölbel, T., Kölbel, L. & Tübke J. (2022). Lithium recovery from geothermal brine- an investigation into the desorption of lithium ions using manganese oxide adsorbents. *Energy Advances* 11, 877-885. DOI:10.1039/d2ya00099g.

IEA. (2024). *Global Critical Minerals Outlook 2024*. IEA, Paris 2024. https://www.iea.org/reports/global-critical-minerals-outlook-2024, Licence: CC BY 4.0

Kang, S., Park, S-M., Park, J-G. & Baek, K. (2019). Enhanced adsorption of arsenic using calcinated alginate bead containing alum sludge from water treatment facilities. *Journal of Environmental Management* 234, 181-188. DOI:10.1016/j.jenvman.2018.12.105.

Lee, J. & Chung, E. (2022). The Effect of Silicate Ions on the Separation of Lithium From Geothermal Fluid. *Frontiers of Chemical Engineering* 4:741281. DOI:10.3389/fceng.2022.741281.

Li, X., Xu, M., Liu, X., She, Q., Lau, W.J. & Yang, L. (2025). Surface-engineered nanofiltration membranes for sustainable lithium recovery from real brine: Addressing fouling and scaling challenges. *Water Research* 278, 123400. DOI:10.1016/j.watres.2025.123400.

Liu, C., Crini, G., Lichtfouse, E., Wilson, L.D., Picos-Corrales, L.A., Balasubramanian, P. & Li, F. (2025). Chitosan-based materials for emerging contaminants removal: Bibliometric analysis, research progress, and directions. *Journal of Water Process Engineering* 71, 107327. DOI:10.1016/j.jwpe.2025.107327.

Mends, E.A. & Chu, P. (2023). Lithium extraction from unconventional aqueous resources- A review on recent technological development for seawater and geothermal brines. *Journal of Environmental Chemical Engineering* 11, 117010. DOI:10.1016/j.jece.2023.110710.

Miao, Q., Jiang, L., Yang, J., Hu, T., Shan, S., Su, H. & Wu, F. (2022). MOF/hydrogel composite-based adsorbents for water treatment: A review. *Journal of Water Process Engineering* 50, 103348. DOI:10.1016/j.jwpe.2022.103348.

Mojid, M.R., Lee, K.J. & You, J. (2024). A review on advances in direct lithium extraction from conventional brines: Ion-sieve adsorption and electrochemical methods for varied Mg/Li ratios. *Sustainable Materials and Technologies* 40, e00923. DOI:10.1016/j.susmat.2024.e00923.

Ningrum, E. O., Murakami, Y., Ohfuka, Y., Gotoh, T. & Sakohara, S. (2014). Investigation of ion adsorption properties of sulfobetaine gel and relationship with its swelling behavior. *Polymer 55*(20), 5189–5197. DOI:10.1016/j.polymer.2014.08.042.

Ningrum, E. O., Purwanto, A., Rosita, G. C. & Bagus, A. (2020). The properties of thermosensitive zwitterionic sulfobetaine NIPAM-co-DMAAPS polymer and the hydrogels: The effects of monomer concentration on the transition temperature and its correlation with the adsorption behavior. *Indonesian Journal of Chemistry 20*(2), 324–335. DOI:10.22146/ijc.41499.

Ningrum, E. O., Safitri, Z. M., Dzaky, M. A., Suprapto, S., Karisma, A. D. & Ni'mah, H. (2022). The effect of temperatures and monomer ratios on the characteristic of anionic and cationic gel-based adsorbents. *IOP Conference Series: Earth and Environmental Science, 963*(1), 012035. DOI:10.1088/1755-1315/963/1/012035.

Ningrum, E. O., Pratiwi, E. L., Shaffitri, I. L., Suprapto, S., Mukti, M. R., Agustiani, E., Puspita, N. F. & Karisma, A. D. (2021). Developments on synthesis and applications of sulfobetaine derivatives: A brief review. *Indonesian Journal of Chemistry 21*(5), 1298–1315.

Recepoğlu, Y.K., Arabaci, B., Kahvecioğlu, A. & Yüksel, A. (2024). Granulation of hydrometallurgically synthesized spinel lithium manganese oxide using cross-linked chitosan for lithium adsorption from water. *Journal of Chromatography A* 1719, 464712. DOI:10.1016/j.chroma.2024.464712.

Reich, R., Danisi, R.M., Kluge, T., Eiche, E. & Kolb, J. (2023). Structural and compositional variation of zeolite 13X in lithium sorption experiments using synthetic solutions and geothermal brine. *Microporous and Mesoporous Materials* 359, 112623. DOI:10.1016/j.micromeso.2023.112623.

Suu, L., Lim, J., Lee, J-H., Choi, Y. & Choi, J-S. (2025). Advances in electrochemical recovery of valuable metals: A focus on lithium. *Desalination* 612, 118960. DOI:10.1016/j.desal.2025.118960.

Tufa, R.A., Santoro, S., Flores-Fernández, C., Zegeye, R.B., Fuentealba, D., Aquino, M., Barraza, B., Inzillo, B.M., Nasirov, S., D'Andrea, G., Troncoso, E., Straface, S., Estay, H. & Curcio, E. (2025). Advances in integrated membrane processes for sustainable lithium extraction. *Desalination* 610, 118899. DOI:10.1016/j.desal.2025.118899.

Weng, D., Duan, H., Hou, Y., Huo, J., Chen, L., Zhang, F. & Wang, J. (2020). Introduction of manganese based lithium-ion Sieve-A review. *Progress in Natural Science: Materials International* 30, 139-152. DOI:10.1016/j.pnsc.2020.01.017.

Wiśniewska, M., Fijałkowska, G., Ostolska, I., Franus, W., Nosal-Wiercińska, A., Tomaszewska, B., Goscianska, J. & Wójcik, G. (2018). Investigations of the possibility of lithium acquisition from geothermal water using natural and synthetic zeolites applying poly(acrylic acid). *Journal of Cleaner Production* 195, 821-830. DOI:10.1016/j.jclepro.2018.05.287.

Wu, M., Wu, L., Zhang, W., Zhong, X., Guo, R., Cui, Z., Yang, Y. & Lv, J. (2025). Efficient removal of cadmium (II) and arsenic (III) from water by nano-zero-valent iron modified biochar-zeolite composite. *Ecotoxicology and Environmental Safety* 296, 118178. DOI:10.1016/j.ecoenv.2025.118178.

Yang, Y., Bi, S., Wang, F., Pan, X., Yang, T., Hu, S., Tang, S. & Jia, Q. (2025). Solid membrane-based aqueous lithium extraction and adsorption: Advances, challenges, and prospects. *Chemical Engineering Journal* 510, 161748. DOI:10.1016/j.cej.2025.161748.

Yuan, H., Li, M., Cui, L., Wang, L. & Cheng, F. (2025). Electrochemical extraction technologies of lithium: Development and challenges. *Desalination* 598, 118419. DOI:10.1016/j.desal.2024.118419.

Zavahir, S., Elmakki, T., Gulied, M., Ahmad, Z., Al-Sulaiti, L., Shon, H.K., Chen, Y., Park, H., Batchelor, B. & Han, D.S. (2021). *Desalination* 500, 114883. DOI:10.1016/j.desal.2020.114883.

Zeng, H., Zeng, Y., Xu, H., Zhao, W., Han, S., Zhang, J. & Li, D. (2024). Selective adsorption of arsenic by water treatment residuals cross-linked chitosan in co-existing oxyanions competition system. *Environmental Research* 263, 120192. DOI:10.1016/j.envres.2024.120192.

Zhou, Y., Tang, X., Qing, D., Li, J. & Wang, H. (2025). Research progress of technology of lithium extraction. *Separation and Purification Technology* 359, 130561. DOI:10.1016/j.seppur.2024.130561.